Chemical Science

Accepted Manuscript

This article can be cited before page numbers have been issued, to do this please use: S. Molla, J. Ahmed and S. Bandyopadhyay, *Chem. Sci.*, 2025, DOI: 10.1039/D5SC02467F.

Chemical Science

Volume 9
Number 1
7 January 2018
Pages 1-268

rsc.li/chemical-science

ISSN 2041-6539

ROYAL SOCIETY OF CHEMISTRY

EDGE ARTICLE
Xinjing Tang *et al.*
Caged circular siRNAs for photomodulation of gene expression in cells and mice

ROYAL SOCIETY OF CHEMISTRY

rsc.li/chemical-science

View Article Online
DOI: 10.1039/D5SC02467F

Double-Anonymised Title Page

Title: All-photonic switching of a benzo[e]-fused dimethyldihydropyrene-azobenzene dyad in solid state for logic operations

Authors:

Sariful Molla[a] Jakir Ahmed[a] and Subhajit Bandyopadhyay*[a]

Affiliations:

[a] S. Molla, J. Ahmed, Prof. S. Bandyopadhyay

Department of Chemical Sciences

Indian Institute of Science Education and Research Kolkata

741246 Mohanpur, Nadia WB, India

E-mail: sb1@iiserkol.ac.in

Acknowledgements:

The authors acknowledge the support by DST-SERB (grant SERB CRG/2022/006776) to S.B. Doctoral fellowship received from CSIR India to S.M. is gratefully acknowledged. J.A. is supported by a fellowship from UGC.

Author contributions:

S.B. initiated the work by conceptualization, funding acquisition, investigation, methodology, resources, writing, and editing. S.M. performed synthesis, photophysical studies. S.M. and J.A. performed the acquisition of the kinetic data and data analysis. The manuscript was written through the contributions of all authors. All authors have approved the final version of the manuscript.

View Article Online
DOI: 10.1039/D5SC02467F

ARTICLE

All-photonic switching of a benzo[e]-fused dimethyldihydropyrene-azobenzene dyad in solid state for logic operations

Received 00th January 20xx,
Accepted 00th January 20xx

DOI: 10.1039/x0xx00000x

Sariful Molla, Jakir Ahmed and Subhajit Bandyopadhyay*[a]

Abstract: Molecular switches offer high-precision tools for achieving photoresponsive control across a wide range of applications, from solar thermal energy storage systems to information processing. Molecular photoswitches are important components for the development of high-density memory devices and photonic information processing. A molecular photoswitch can generate at least two distinct states. Photochromic dyads of coupled photoswitches can attain more than two states if the two switches are independently addressable. However, orthogonal photoswitching in hybrid photochromic systems could be challenging. In this work, we discuss the development of two orthogonal hybrid photochromic dyads, integrating two distinct photoswitches: dimethyldihydropyrene (DHP) or benzo[e]-fused dimethyldihydropyrene (BDHP) with azobenzene. Despite the significant spectral overlap between these systems, careful design and selection of suitable light sources ranging from NIR to UV light have successfully decoupled the individual photoswitching processes. As a result, four well-characterized distinct states can be selectively controlled with light. We have constructed an all-photonic molecular logic gate by switching the system in thin film, showcasing the potential of these systems for advanced molecular information processing using the attenuated total reflectance (ATR)-based FTIR spectroscopy as the non-destructive readout mode.

Introduction

Given the precise control of ON/OFF activity in different environments ranging from large macroscale to nanostructure properties, molecular switches have gained much attention in recent years.[1-6] Particularly, the use of light as an external stimulus is of key importance because of its non-invasive nature and its ability to control the processes both in terms of precise 3D space and time. Moreover, light does not generate any byproduct, unlike a chemical stimulus such as protons.[7] Control of various processes in chemical research starting from catalysis,[8-11] photopharmacology,[12-15] super-resolution fluorescence imaging,[16-19] energy storage materials[20-24] to the construction of molecular logic gates[25-28] can be controlled reversibly by photochromic switches such as stilbene, azobenzene, diarylethene, or dimethyldihydropyrene. A major advancement in the field with the emergence of several new generation of photoswitches including modified indigos,[29-32], all-visible light enabled azobenzenes,[33-36] heteroaryl azoswitches,[37-40] donor-acceptor adducts (DASA),[41-43] imidazole dimers[44-46] and photoswitchable imines[47-49] has provided a new impetus to the field. These monomeric photoswitches offer an ON/OFF binary response depending on the wavelength of the light used for the irradiation. However, the complexity of advanced devices demands the development of multi-responsive systems with more than two addressable states. In this regard, the emergence of multi-photochromic systems have offered novel solutions to the problem.[25,50-54] Ideally, a multi-photochromic compound consisting of two photoswitches (dyad) generates 2^2 states of a molecule. A molecule, thus, having n-photoswitches, can generate 2^n states. To elicit the functions of the photoswitchable components in a multi-switch, each of the photoswitchable units of the molecule needs to be driven by orthogonal light sources that offer selective addressability of the individual states. To establish an all-photon photochromic system consisting of two components, at least four different lights are needed for the molecule to provide controllable access and selectively yield all four distinct states (Fig. 1). To make use of those states, it is desirable that these states are long-lived and stable under ambient conditions. Also, the efficiency of each photoconversion is determined by the composition of the photostationary states (PSS); a quantitative conversion, earmarked by a high PSS, results in more exclusive features with higher purity of a particular state. Achieving wavelength-orthogonality in photoswitchable dyad requires distinct spectral separation for each constituent switch. However, among the available molecular photoswitches, such as stilbene, azobenzene, dimethyldihydropyrene, diarylethenes, and spiropyrans have

---

*[a] S. Molla, J. Ahmed, Prof. S. Bandyopadhyay
Department of Chemical Sciences
Indian Institute of Science Education and Research Kolkata
741246 Mohanpur, Nadia WB, India
E-mail: sb1@iiserkol.ac.in*

Supplementary Information available: [details of any supplementary information available should be included here]. See DOI: 10.1039/x0xx00000x

View Article Online
DOI: 10.1039/D5SC02467E

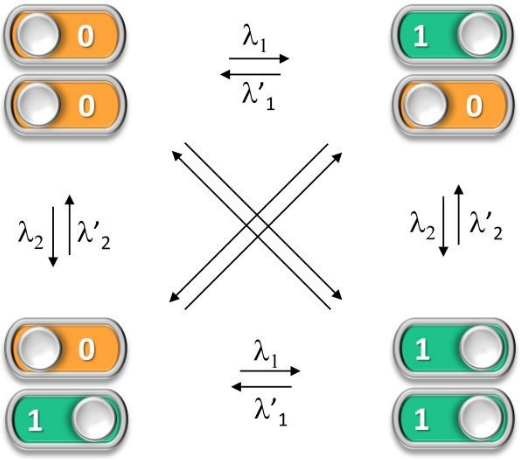

Fig. 1 Multistate Photoswitching in an ideal photochromic dyad. The isomerization between the two diagonal states would require a combination of two different wavelengths of light.

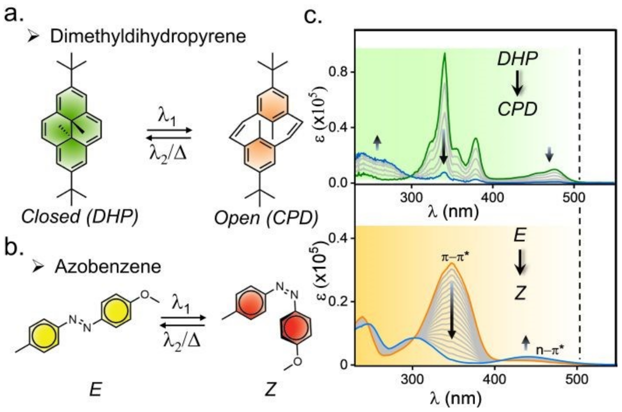

Fig. 2 a) Molecular structure and switching of Dimethyldihydropyrene (DHP) and b) Azobenzene; c) Absorbance spectra of DHP and Azobenzene, and the spectra upon isomerization, showcasing overlapping of the spectrum ranging from 230 nm to 510 nm in CH_3CN.

significant spectral overlap in the ultraviolet region.[3,55-58] Thus, making it difficult to design a multi-photoswitch system constituting these molecular switches. Recently, notable advancements have been made to achieve path independent orthogonal photoswitching, but many of them require incorporation of a secondary stimuli like a thermal[50,59-61], electrical, or chemical[62,63] isomerization process to achieve orthogonality. In this work, we have established an all-photon, wavelength-selective orthogonal photoswitching combining two photochromic systems classes. The dimethyldihydropyrene (DHP) and azobenzene overlap in the UV-visible spectrum and use almost the same wavelengths of light for photochemical isomerization (Fig. 2a-c). This makes it almost impossible to develop a hybrid photochromic dyad consisting of these two photoswitches that can be controlled orthogonally. To overcome this challenge, we have executed synthetic modifications on parent DHP, which caused a red-shifted UV-visible spectrum, ultimately making selective excitation possible. DHP, upon isomerization, can also react with molecular oxygen, reducing the photochromic efficiency.[64,65] Again, synthetic measures have been taken to improve the switching efficiency both in water and thin films. The orthogonally photo-addressable states feature enabled the demonstration of a molecular logic device. Molecular logic gates are the prototypes for developing molecular information storage or molecular computing devices. As the hybrid systems satisfy the fundamental requirements to establish a molecular logic gate, a) the output or the responses are distinctly observable, b) the response is very fast, and c) the reversibility or the ability to run multiple cycles without visible fatigueness.[66,67] In this context, several readout method-based molecular logic gates are there; for example, absorbance[68] probe-based, fluorescence[69] output-based, and more recently, a SERS[70] output-based molecular logic gate has been developed. All these methods have their advantages and disadvantages. ATR-FTIR spectroscopy has never been used for molecular logic representations. The huge advantage of ATR measurement is that it does not require extensive sample preparation; a high-quality IR spectrum can be obtained from a simple drop-casted sample. To the best of our knowledge, this is the first example of the ATR FT-IR spectrum-based molecular logic operations.

Results and discussion

The orthogonal photochromic systems discussed here consist of a dimethyldihydropyrene (DHP), a negative photochromic system, and azobenzene, a positive photochromic system, each utilizing distinct photoisomerization mechanisms. Our initial investigations focused on a relatively simple system **1**, where DHP and azobenzene are electronically conjugated (Fig. 3). A Suzuki-Miyaura coupling reaction gave the final derivative (see supporting information for synthetic details). The two UV/Vis responsive photoswitches are electronically connected and display a red-shifted absorption spectrum. The absorption spectrum suggests significant overlap between the two switches, with DHP exhibiting a higher molar extinction coefficient. Consequently, the absorption spectrum of **1** is

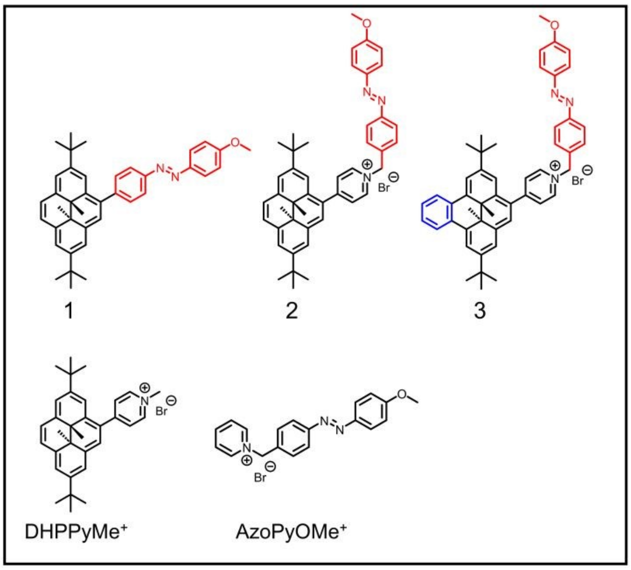

Fig. 3 Studied derivatives.

View Article Online
DOI: 10.1039/D5SC02467F

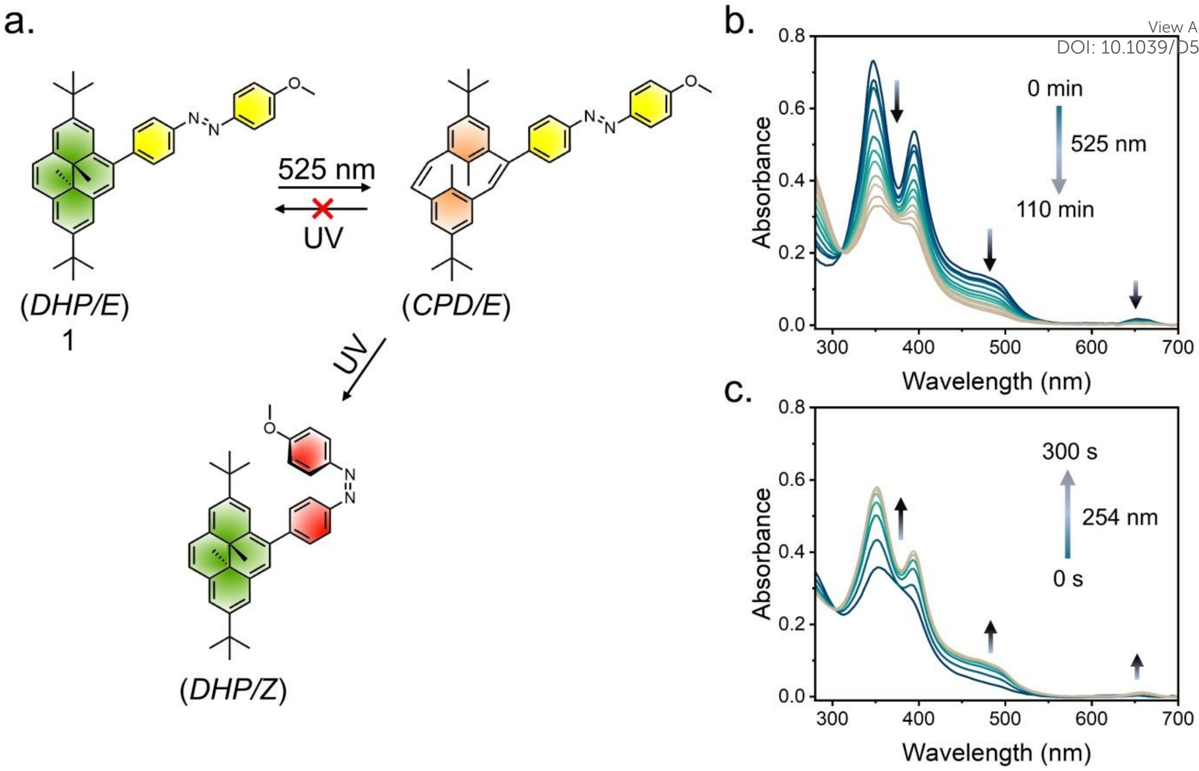

Fig. 4 a) Schematic of photoisomerization upon irradiation of different lights in derivative **1**. Changes in UV/Vis absorbance spectra from b) Closed to open (*DHP→CPD*) isomerization of the DHP unit selectively. c) Showcasing both ring-closing of DHP (*CPD→DHP*) and *E→Z* isomerization of the azobenzene component upon UV light irradiation.

primarily dominated by the π-π* transitions of DHP. To selectively induce the *DHP→CPD* isomerization while leaving the azobenzene unit unaltered, **1** was irradiated with 525 nm visible light. This resulted in a significant hypsochromic shift in the UV/Vis spectrum, indicating the opening of the highly conjugated aromatic ring (*DHP*/*E* → *CPD*/*E*) (Fig. 4a, b). The quantum yield (f) of 1.6×10^{-4} (f_{525nm}) for the ring-opening photoisomerization, which is quite low, as it took approximately 107 minutes to reach the corresponding PSS (Fig. S27, Table S1). Also, the challenge arises during the reversal of this isomerization, as UV light not only reverses the *CPD→DHP* isomerization but also triggers the *E→Z* isomerization of azobenzene simultaneously (Fig. 4c, Fig. S24c). However, Selective reversal of the *CPD→DHP* isomerization can be achieved through thermal treatment, which preserves the *E*-isomer of azobenzene. However, to fully reverse the *CPD* system, heating a 10 µM solution in CH_3CN at 70°C requires approximately 40 minutes (Fig. S22). While effective, thermal treatment is an invasive stimulus and requires a prolonged duration, making it impractical for many real-world applications. Thus, alternative, faster, and less invasive methods are needed to improve the efficiency and applicability of the system. To address these challenges and develop an orthogonally operating, all-photon photochromic hybrid system, we revisited the literature. Royal and coworkers recently demonstrated that the incorporation of strong electron-withdrawing groups results in a significant red shift in the absorption spectrum, enabling blue light-induced ring closure (*CPD→DHP*).[71,72] To selectively reverse the open CPD ring to its closed DHP form in a DHP-azobenzene coupled system, it is essential to achieve visible light-mediated *CPD→DHP* ring-closing. The details of the design principle of the hybrid switch are discussed below. To select the suitable DHP switch, a model derivative, **DHPPyMe⁺**, was synthesized with **Br⁻** as a counter anion. In comparison to the parent DHP, in CH_3CN, **DHPPyMe⁺** has showcased a significantly red-shifted UV/Vis absorption spectrum with distinct π-π* bands around 339 nm

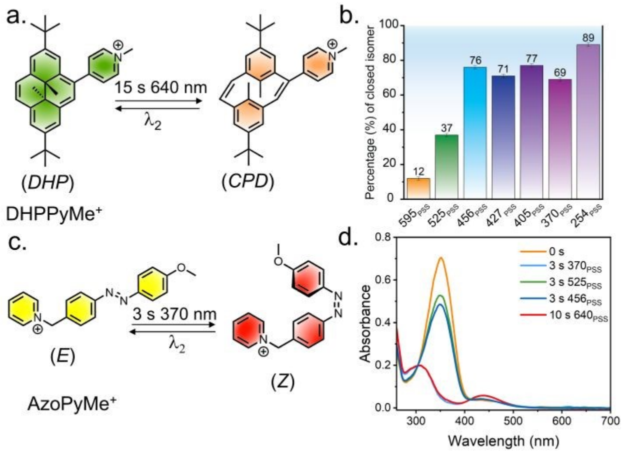

Fig. 5 a) Molecular structure of DHP with attached pyridinium acceptor. b) Percentage of ring closed isomer obtained during reverse isomerization for **DHPPyMe⁺**. Showing PSS upon illumination with lights of different wavelength. c) Molecular structure of azobenzene derivative for control studies. d) UV absorbance spectra of **AzoPyMe⁺** upon irradiation of different lights. All the above-mentioned solution state studies were done in acetonitrile solution (10 µM, 298 K).

View Article Online
DOI: 10.1039/D5SC02467F

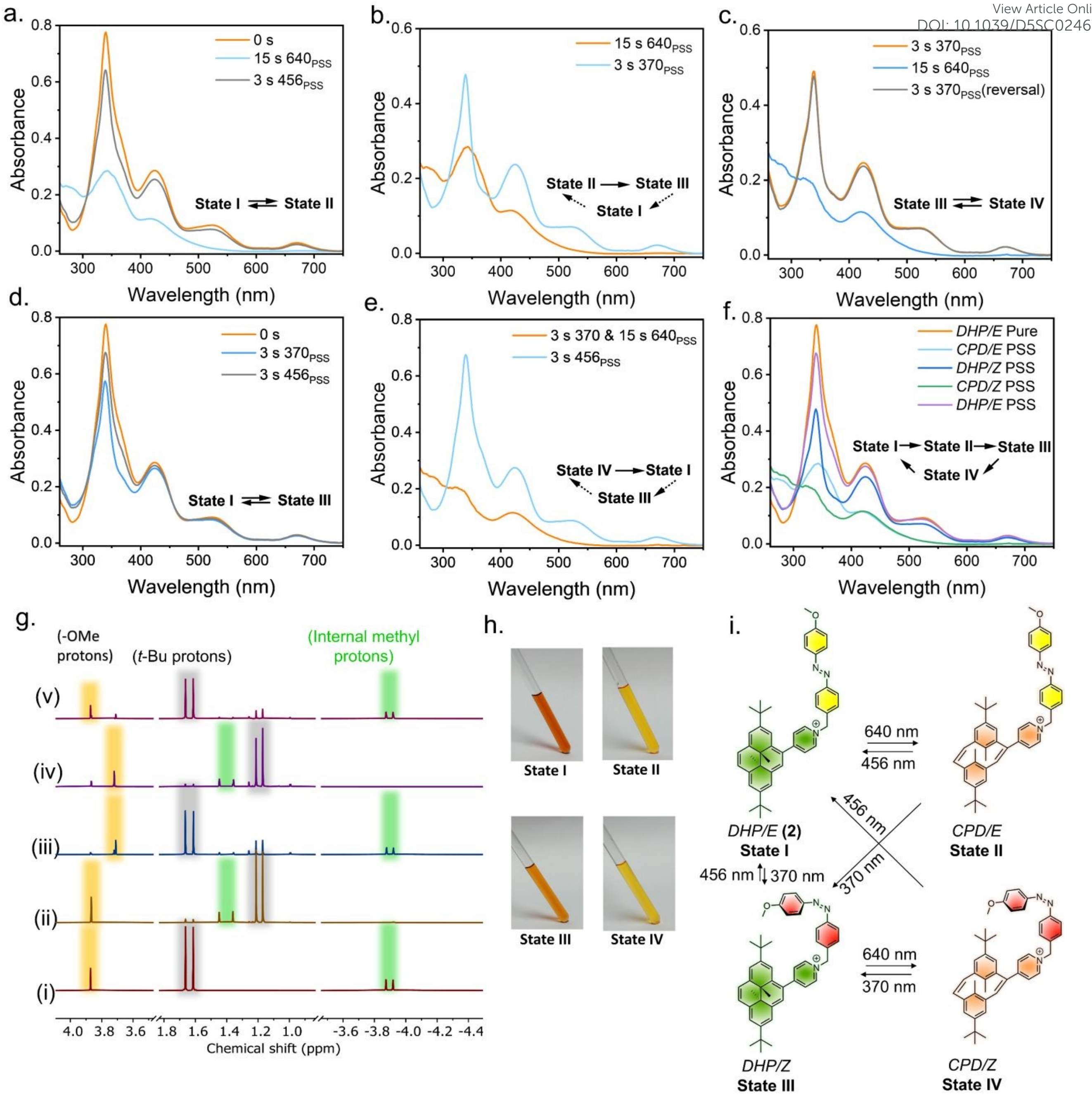

Fig. 6 a) Reversible and orthogonal isomerization of DHP (*DHP*/*CPD*) without affecting the azobenzene switch by irradiation of 640 nm for 15 s and 456 nm for 3 s. b) Simultaneous switching of DHP (*CPD*→*DHP*) and azobenzene (*E*→*Z*) by 370 nm for 3 s. c) Reversible control of the DHP/CPD isomerization keeping *Z*-isomer of azobenzene intact by 640 nm for 15 s and 370 nm for 3 s. d) Reversible and orthogonal control of azobenzene switching (*E*/*Z*) without affecting the DHP switch by alternate irradiation of 370 nm (*E*→*Z*) and 456 nm (*Z*→*E*) for 3 s. e) Simultaneous reversal of *CPD*/*Z*→*DHP*/*E* by 456 nm for 3 s. f) Sequential control of different states and the corresponding spectrums of PSS achieved by different wavelengths of light irradiation. g) Orthogonal photoswitching monitored by ^{1}H NMR (400 MHz, CD_3CN, 298 K) studies with a 50 mM solution (i) before irradiation (**State I**), (ii) PSS of **State II** depicting shift of internal methyl protons (green) and *t*-Bu protons (grey). (iii) PSS of **State III** highlighting the *E*→*Z* isomerization of the azobenzene with shift of methoxy proton (yellow). (iv) PSS of **State IV**, (v) Recovery of **State I** with a PSS. h) Photographs of **2** in different states in solution of 50 mM (CD_3CN). Changes in UV/Vis spectrum upon photoexcitation of light at selective wavelengths i) Schematic representing all the possible all-photon orthogonal photoswitching achieved using a combination of DHP-Azobenzene coupled system with high PSS.

(ε = 71600 $M^{-1}cm^{-1}$), 415 nm (ε = 34000 $M^{-1}cm^{-1}$), 505 nm (ε = 11100 $M^{-1}cm^{-1}$), 665 nm (ε = 3200 $M^{-1}cm^{-1}$). **DHPPyMe⁺** can be photoisomerized with red light (640 nm), and excitation with 640 nm light in a degassed solution of CH_3CN (10 μM) yielded the corresponding open isomer quantitively (Fig. 5a, b). The strong absorption bands in the visible region disappear, giving a colorless solution, a signature of negative photochromism. To determine a suitable visible light wavelength for reversing the open isomer, different light sources were tested. Although 254 nm UV light achieved the best PSS (89%), enriching **DHPPyMe⁺**, irradiation with 456 nm light also significantly enriched the closed isomer, reaching a PSS of 76% (Fig. S23). The visible light

View Article Online
DOI: 10.1039/D5SC02467F

(456 nm) mediated reversal of open isomer to **DHPPyMe$^+$** was further confirmed by ^{1}H NMR spectroscopy (Fig. S24a). This suggests that 456 nm light can be employed for DHP ring-closing in systems containing strong electron-withdrawing groups, such as the pyridinium cation. To understand the effect of 456 nm and 640 nm light on azobenzene, we have synthesized a control azobenzene derivative, **AzoPyMe$^+$**. 525 nm and 456 nm irradiation caused a minor *E*→*Z* isomerization of the azobenzene unit, whereas 640 nm did not cause any isomerization, as confirmed by control experiments using only azobenzene (Fig. 5c, d, S24b). Therefore, putting all the points into perspective, we have synthesized a modified DHP and azobenzene coupled photochromic dyad derivative 2 with a strategic inclusion of pyridinium cationic moiety (see supporting information for synthetic details). Since DHP has a high molar extinction coefficient, the absorption spectrum is mainly dominated by the π-π* bands of the DHP. The UV-Vis spectrum of **2** exposed four distinct absorption bands at around 340 nm (ε = 77600 M^{-1}cm^{-1}), 425 nm (ε = 28500 M^{-1}cm^{-1}), 525 nm (ε = 9100 M^{-1}cm^{-1}), and 670 nm (ε = 2800 M^{-1}cm^{-1}) in 10 μM CH_3CN. Irradiation with 640 nm light leads to a significant blue shift of the absorption bands, accompanied by an increase of the band intensity in the shorter wavelength region (ca. 270 nm). Consistent with the ring opening (*DHP*→*CPD*) photoisomerization of the DHP unit (Fig. 6a). The reduction of the band intensity at the longer wavelength region is attributed to breaking a highly conjugated aromatic 14π-electron system into two discrete 6π-electron systems. Visually, the deep orange-colored solution bleached into a yellowish solution (Fig. 6h). The selective ring opening of DHP from *DHP*/*E*(**State I**)→*CPD*/*E*(**State II**) was confirmed from the ^{1}H-NMR isomerization measurements in CD_3CN, in *DHP*/*E*, DHP being in its closed isomeric form, exhibits a characteristic chemical shift for the internal methyl protons, which is around -3.87 ppm, and the disruption of the aromatic DHP to CPD led these protons shifted to +1.4 ppm along with significant shift of the *t*-Bu and other aromatic protons (Fig. 6g). The methoxy (OMe) protons are unaffected, indicating quantitative ring opening without affecting azobenzene. To probe whether the 456 nm light-enabled reversal of DHP could be retained in a coupled system or to achieve *CPD*/*E*→*DHP*/*E* reversal, we have subjected the sample to 456 nm light irradiation on the *CPD*/*E* (**State II**) isomer. Exposure for 3 s led to the reappearance of the characteristic UV/Vis absorption bands of the closed isomer, suggesting ring closing of the DHP unit (Fig. 6a). The selective ring closing (*CPD*/*E*→*DHP*/*E*) is accompanied by the recurrence of the orange color of the solution (Fig. 6h). However, it is important to note that 456 nm light caused a minor degree of *E*→*Z* isomerization of the azobenzene unit, likely due to the red shift in the UV-Vis spectrum. ^{1}H NMR spectroscopy corroborated the selective *CPD*→*DHP* isomerization, with the reappearance of the −3.87 ppm peak along with a small peak at 3.70 ppm, corresponding to the methoxy protons of the *Z*-isomer, indicating some degree (30%) of *E*→*Z* conversion of the azobenzene unit (Fig. 6g). This observation is in accordance with the reference derivative **AzoPyMe$^+$,** which showed minor *E*→*Z* isomerization under 456 nm irradiation (Fig. 5d). Subsequent irradiation with 370 nm light to the *CPD*/*E* isomer (**State II**) led to the back *CPD*→*DHP* isomerization of the DHP unit accompanied by the *E*→*Z* isomerization of the azobenzene (**State II→State III**). The reduced intensity of UV/Vis absorbance band (*ca.* 370 nm) is observed because the π-π* absorption band of azobenzene also resides in this region, and upon *E*→*Z* isomerization the absorbance of this band decreases, and as a whole, reduced intensity is observed (Fig. 6b). The orange color of the solution also comes back. The major changes that have been observed in the ^{1}H NMR are the shift of the -OMe protons from 3.86 ppm to 3.70 ppm, suggesting *E*→*Z* isomerization, along with changes for the *CPD*→*DHP* isomerization that has been stated previously. (Fig. 6g) Again, back-to-back irradiation of 456 nm for 3 s and 640 nm light for 15 s gave back the *CPD*/*E* isomer (**State II**) by following the path **State III** → **State I** → **State II.** Excitation of *DHP*/*Z* isomer (**State III**) with 456 nm for 3 s resulted in spectral changes in the shorter wavelength region only, suggesting the *Z*→*E* isomerization of the azobenzene without affecting the DHP, thereby directly reaching **State I** from **State III** (Fig. 6b). Alternatively, irradiation of 370 nm on *Closed-Cis* isomer (**State I**) for 3 s led to the decrease in absorbance at λ=370 nm, indicating the reversal of the azobenzene to the *Z*-isomer (*E*→*Z*) (**State I→State III**) (Fig. 6d). ^{1}H NMR isomerization also revealed the shift of the methoxy (-OMe) protons only by keeping other protons associated with DHP intact, indicating *E*→*Z* isomerization (Fig. 6g). Therefore, irradiation with 640 nm of the *DHP*/*Z* isomer (**State III**), the characteristic bands of DHP gradually disappear, indicating the *DHP*→*CPD* ring opening while keeping azobenzene in its E/*Z*-PSS intact, thereby giving rise to the **State IV**, enriched with *CPD*/*Z* isomer. Subsequent irradiation with the 370 nm light source resulted in the recovery of **State III**, the majority of the azobenzene units already being in *Z*-form; only the DHP undergoes *CPD*→*DHP* isomerization (Fig. 6c). The changes were further examined by ^{1}H NMR spectroscopy, and the corresponding PSS compositions were evaluated (Fig. 6g). The **State I** can be recovered from **State IV**, upon subsequent irradiation of **State IV** at 456 nm led to the isomerization of both the switches, for DHP (*CPD*→*DHP*) and azobenzene (*Z*→*E*) (**State IV→State I**). The UV/Vis spectral changes are consistent with the characteristic bands of DHP, and the increase of the absorbance centered at around 370 nm compared to the *DHP*/*Z* isomer (**State III**) indicates *Z*→*E* isomerization of azobenzene (Fig. 6e). The result obtained through irradiation of **State IV** at 456 nm is also consistent with **State III→State I** or **State II→State I** transformations (Fig. 6e, d). Similarly, another possibility is **State IV→State I→State III** (Fig. 6e). To showcase the sequential generation of multiple states, we tried generating each state by changing light source only in one go, one after the other: the sequential and consecutive irradiation of 640 nm→370 nm→640nm→456 nm generated four different isomeric states and then again recovered to the initial state, in the order **State I→State II→State III→State IV→State I** (Fig. 6f). Therefore, the strategically designed DHP-azobenzene coupled photochromic systems can be orthogonally switched and used in advanced devices for multi-responsive operations despite having a large overlap in the UV/Vis spectrum of the operating

View Article Online
DOI: 10.1039/D5SC02467F

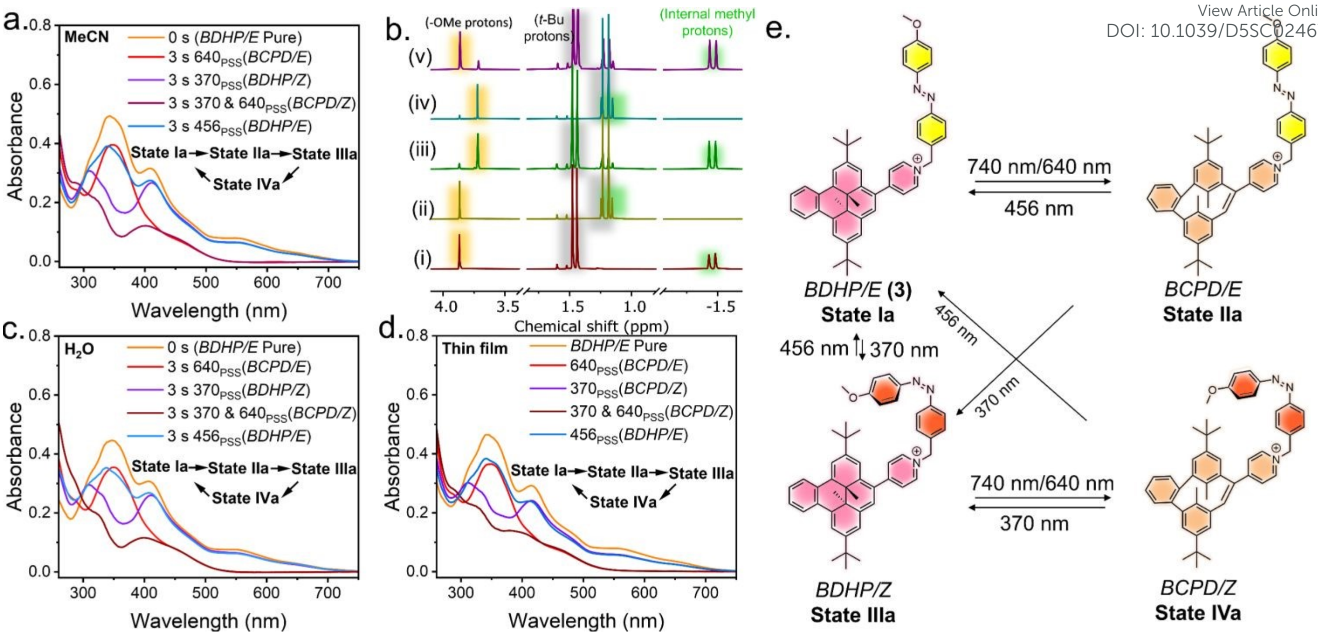

Fig. 7 a) Sequential control of different states and the corresponding absorbance spectrums of PSS achieved by different wavelengths of light irradiation in MeCN (10 μM). b) Orthogonal photoswitching monitored by ^{1}H NMR (400 MHz, CD_3CN, 298 K) studies with a 50 mM solution (i) before irradiation (**State Ia**), (ii) PSS of **State IIa** depicting shift of internal methyl protons (green) and *t*-Bu protons (grey). (iii) PSS of **State IIIa** highlighting the *E→Z* isomerization of the azobenzene with shift of methoxy protons (yellow). (iv) PSS of **State IVa**, (v) Recovery of **State Ia** with a PSS. Sequential control of different states and the corresponding spectrums of PSS achieved by different wavelengths of light irradiation c) in H_2O (10 μM). d) in drop casted thin film. e) Schematic representing all the possible all-photon orthogonal photoswitching achieved using a combination of BDHP-Azobenzene coupled system with high PSS.

region (Fig. 6i). The above system has a few drawbacks that are described as follows. a) The ring opening quantum yield for the DHP using 640 nm light is low (Fig. S27, Table S1). Therefore, a 10 mm solution in CH_3CN takes almost 15 s for *DHP→CPD* isomerization; b) The photochemical ring opening in aerobic conditions has led to the formation of unwanted endoperoxide derivatives, thereby decreasing the efficiency of the hybrid switching cycles. During fatigue resistance studies of derivative **2,** we found that whenever there is a switching step involving DHP↔CPD isomerization that shows a gradual decay in photostability (Fig. S25). We have also been able to identify the formation of the corresponding endoperoxide for derivative **2** by high resolution mass spectrometry (HRMS), where the experimentally observed pattern matched with the simulated pattern (Fig. S21), consistent with the literature reports of endoperoxides of the DHP pyridinium salts.[64,65] In order to overcome the disadvantages faced with **2**, we synthesized the benzo[e]-fused dimethyldihydropyrene (BDHP) that switches much faster with better efficiency, and also does not react with O_2, devoid of any such endoperoxide formation or degradation even after multiple cycles; hence, flawless switching of BDHP in aerobic conditions is expected.[64] The benzo[e]-fused

Table 1. PSS achieved upon consecutive irradiation of different wavelengths of light.

Compounds	PSS at different wavelengths of light, λ (nm)				
	Before irradiation	640 nm	370 nm	640 nm	456 nm
2	State I (DHP/E) 100:100	State I →State II (CPD/E) 98/100	State II → State III (DHP/Z) 72/95	State III → State IV (CPD/Z) 97/92	State IV → State I (DHP/70) 71:70
3	**State Ia** **(BDHP/E)** **100:100**	**State Ia → State IIa** **(BCPD/E)** **99/100**	**State IIa → State IIIa** **(BDHP/Z)** **81/94**	**State IIIa → State IVa** **(BCPD/Z)** **98/93**	**State IVa → State Ia** **(BDHP/E)** **80:71**

[a] PSS: Photostationary State. [b] The PSS were determined from the ^{1}H NMR isomerization studies in 50 mM CD_3CN solution.

dimethyldihydropyrene was synthesized following the literature,[73] and subsequently **3** as its **Br**$^-$ salt was synthesized by following the similar steps as **2** (see the supporting information for more details). The tail of the absorbance of **3** extends up to ~750 nm (Fig. 7a). Unlike derivative **2**, the π-π^* transition of the azobenzene moiety has a significant contribution to the UV/Vis spectrum of **3**. This increased contribution becomes evident during the switching process, where significant absorbance changes are observed due to the *E*/*Z* isomerization of azobenzene. The transition from **State I** to **State II** for **2**, corresponding to the *DHP→CPD* ring opening took approximately 15 seconds when irradiated with 640 nm light in a 10 µM CH_3CN solution. In contrast, for **3**, this process is significantly accelerated, requiring only 3 seconds of irradiation, indicating a marked enhancement in the photoisomerization quantum yield. It is important to note that the absorbance tail of **3** extends nearly to 750 nm, allowing for ring opening (**State Ia→State IIa**) using a 740 nm light source, although it takes around 15 seconds due to the significant lowering of molar extinction coefficient at 740 nm (Fig. 7a). The remaining UV/Vis isomerization studies align with our previous findings of derivative **2** and follow the same trend. Multiple switching cycles of each state were performed, and the isomerization showed little to no decay in photochromic efficiency, which ensured the robustness and the fatigue-resistant properties of **3** (Fig. S26). The PSS distributions of each step were further evaluated by ^{1}H NMR isomerization studies (Fig. 7b). The PSS distribution for each of the states improved for **3** compared to **2** (Table 1), which is attributed to the red shift of the BDHP chromophore compared to the parent DHP, leading to better decoupling with azobenzene spectrum. Both DHP/BDHP and azobenzene belong to the category of T-type photoswitch, i.e., the photogenerated species can return to the stable isomer under heating or dark depending on the reaction's activation energy (*Ea*). Therefore, to investigate the stability of the photogenerated states, we have performed variable temperature studies for derivative **3** (Fig. S28, S29, S31). Kinetic measurements revealed that the E_a for *BCPD→BDHP* is 19.8±0.5 Kcal.mol^{-1} and the half-life ($t_{1/2}$) 9.5h, for *Z→E* thermal reversal, the E_a is 25.3±0.5 Kcal.mol^{-1} and $t_{1/2}$ almost 53h (Fig. S30, S32, Table S2). The above results suggest that the photogenerated states are highly stable, which is a necessary criterion for using these photo-addressable states. Both the derivatives **2** and **3** were found to be water soluble with its **Br**$^-$ counter anion, and thus, we investigated photochromic properties in an aqueous medium. The photoswitching properties of **3** in the water (10 mM) by UV/Vis spectroscopy revealed that all four states can be achieved without any significant decay in the photochromic efficiency (Fig. 7c). For almost all types of device applications, it is essential to have photoswitching ability in solvent-free conditions. We have monitored the light-mediated absorbance changes in a drop-cast thin film and compared it with the switching in solution (CH_3CN) (Fig. 7d, Fig. S33). The comparable absorbance spectra of each state suggest that the switching properties have been retained in thin film. Thus, the work presents the development of a multistate addressable photochromic dyad that is robust and compatible in the aqueous media and thin films for smart devices or practical applications (Fig. 7e). To explore the possibility of ATR FTIR signal output-based molecular logic gate, the FTIR spectra of the derivative **3** and all the light-generated states were recorded (Fig. 8a), and the spectrum bands were analyzed to identify the signals that undergo change upon isomerization. The FTIR spectra were recorded on drop-cast and dried samples. The light-gated forward and reverse switching provides two different wavelengths of light as input and the acquired FTIR bands as output, which can be utilized to formulate a logic gate. The bands at 1537 cm^{-1} and 1140 cm^{-1} have showcased state-specific vibrations. The derivative **3,** in its pristine state, when no light was applied (both input **A** = 0 and input **B** = 0), the **State Ia** (pure *BDHP/E* form) exhibited no band at 1537 cm^{-1} but had a signal at 1140 cm^{-1}. Upon interconversion to **State IIa** (*BCPD/E*) with 640 nm light (i.e., inputs are **A** = 1 and **B** = 0), a band at 1537 cm^{-1} appeared, and the signal at 1140 cm^{-1} remained unchanged. When we irradiated the sample with only 370 nm wavelength of light (i.e., input **A** = 0 and input **B** = 1), we achieved **State IIIa** (*BDHP/Z*), where both the signals at 1537 cm^{-1} and 1140 cm^{-1} were absent. Subsequently, upon exposure to both 640 nm and 370 nm light (i.e., when both inputs are **A** = 1 and **B** = 1), it gave another state, **State IVa** (*BCPD/Z*), and only the vibration signal at 1537 cm^{-1} reappeared, but the band at 1140 cm^{-1} remained low in intensity. Based on the above analysis of the signals at 1537 cm^{-1} and 1140 cm^{-1}, it is clear that the ring opening of the BDHP component (*BDHP→BCPD*) is responsible for the appearance of the 1537 cm^{-1} signal and the

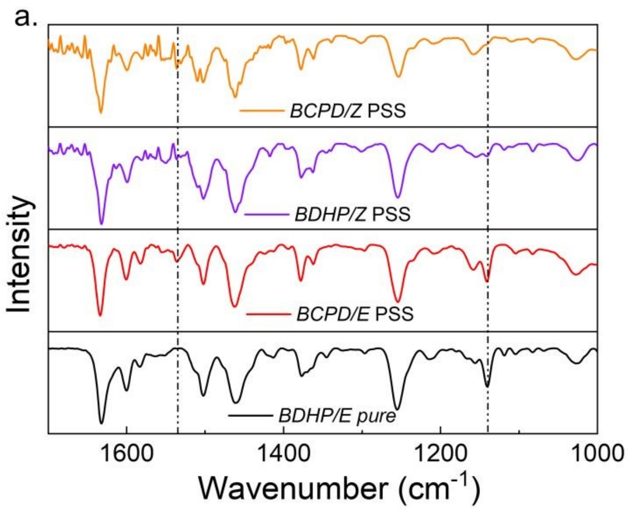

b.

Inputs		Output	
640 nm (A)	370 nm (B)	YES (1537 cm^{-1})	NOT B (1140 cm^{-1})
0	0	0	1
1	0	1	1
0	1	0	0
1	1	1	0

Fig. 8 a) Experimental ATR FTIR spectra of derivative **3** in pristine state and other photogenerated states. b) I/O Truth table representing the optical input and FTIR signal as output.

View Article Online
DOI: 10.1039/D5SC02467F

E isomeric form of the azobenzene component is responsible for the 1140 cm^{-1} signal. Therefore, the *E*→*Z* isomerization caused the disappearance of the 1140 cm^{-1} peak. These configurations suggest that two different logic gates can be operated. The input-output (I/O) truth table has revealed that the information can be represented as YES and NOT B logic gates by monitoring 1537 cm^{-1} and 1140 cm^{-1} peaks (Fig. 8b).

Conclusions

In summary, we present a novel all-photon stimuli-responsive orthogonal photochromic dyad consisting of a dimethyldihydropyrene type (DHP/BDHP) and methoxy-substituted azobenzene. Notably, the orthogonality could not be achieved by simple coupling of the photoswitches due to the high overlapping of the photochemically active region of the UV/Vis spectrum. However, a rational structural modification led to the significant bathochromic shift of the absorption spectra, particularly affecting the switching wavelengths of DHP/BDHP, allowing visible light-mediated reversal, and ultimately decoupling the activities of two photoswitches so that they can be switched independently. However, two disadvantages of a pyridinium cation attached to DHP seemed problematic: a) low photoisomerization quantum yield and b) O_2 sensitization, thereby decreasing the photochromic efficiency. These were addressed and solved in derivative **3** where the photoisomerization quantum yield increased, and the compound was inactive towards O_2. Therefore, multiple cycles of switching can be achieved, ensuring its fatigue resistance. Interestingly, the substitution of the DHP with the benzo[e]-fused dimethyldihydropyrene has led to a further red shift of the UV/Vis spectra, which enabled NIR light (740 nm) mediated ring opening (**State Ia**→**State IIa**) as well as improved PSS of each addressable states. The switching property has been demonstrated in thin films as well. Inspired by the results and the robustness of the compound in air and moisture, we explored this dyad system for all-photonic multi-addressable logic applications. ATR based FTIR spectrum was used as a non-destructive readout mode for the logic operations. We believe that an easy, cost effective and non-destructive readout method like ATR FTIR might open up a plethora of future applications in molecular computing technology.

Author contributions

The manuscript was written through the contributions of all authors. All authors have given approval to the final version of the manuscript.

Conflicts of interest

There are no conflicts to declare.

Data availability

The data that support the findings of this study are available in the Supporting Information of this article.

Acknowledgements

The authors acknowledge the support by DST-SERB (grant SERB CRG/2022/006776) to S. B. Doctoral fellowship received from CSIR India to S.M. is gratefully acknowledged. J.A. is supported by a fellowship from UGC.

Notes and references

‡ Footnotes relating to the main text should appear here. These might include comments relevant not central to the matter under discussion, limited experimental and spectral data, and crystallographic data.
§
§§
etc.

1 M. M. Russew and S. Hecht, *Adv. Mater.*, 2010, **22**, 3348–3360.
2 C. Brieke, F. Rohrbach, A. Gottschalk, G. Mayer and A. Heckel, *Angew. Chemie - Int. Ed.*, 2012, **51**, 8446–8476.
3 B. L. Feringa, W. R. Browne, N. R. Branda, S. Bronco, F. Ciardelli, A. Credi, F. Diederich, J. H. van Esch, L. Fabbrizzi, J. Frey, E. Friedrichs, R. Gomes, T. Gushiken, K. Ichimura, J. de Jong, W. Knoll, V. Lemieux, P. Liljeroth, M. Maesri, C. R. Mendonca, V. I. Minkin, S. J. van der Molen, O. N. Oliveira Jr., A. J. Parola, O. Pieroni, F. Pina, A. Pucci, F. M. Raymo, D. S. dos Santos Jr., Z. Sekkat, J. P. Sauvage, T. Seki, M. Semerano, A. P. de Silva, F. C. Simmel, C. Tock, H. Tian, M. Tomasulo, D. Trauner, T. Ubukata, T. P. Vance, M. Venturi, M. Volgraf, Q.-C. Wang, B. Wannalerse, C. C. Warford, M. E. S. West, Y. Yokoyama and V. Zucolotto, Molecular Switches, Wiley-VCH, Weinheim, 2011.
4 S. Iamsaard, S. J. Aßhoff, B. Matt, T. Kudernac, J. J. L. M. Cornelissen, S. P. Fletcher and N. Katsonis, *Nat. Chem.*, 2014, **6**, 229–235.
5 Q. Qi, J. T. Plank, A. R. Lippert and I. Aprahamian, *Chem* 2024, **10**, 3575–3581.
6 T. Tran Ngoc, N. Grabicki, E. Irran, O. Dumele and J. F. Teichert, *Nat. Chem.*, 2023, **15**, 377–385.
7 Z. L. Pianowski, *B. L. Feringa, Molecular Photoswitches: Chemistry, Properties, and Applications, 2 Volume Set.*, Wiley-VCH. 2022.
8 R. G. DiNardi, S. Rasheed, S. S. Capomolla, M. H. Chak, I. A. Middleton, L. K. Macreadie, J. P. Violi, W. A. Donald, P. J. Lusby and J. E. Beves, *J. Am. Chem. Soc.*, 2024, **146**, 21196–21202.
9 R. Göstl, A. Senf and S. Hecht, *Chem. Soc. Rev.*, 2014, **43**, 1982–1996.
10 M. Saha, M. S. Hossain and S. Bandyopadhyay, *Angew. Chemie - Int. Ed.*, 2021, **60**, 5220–5224.
11 G. Sobczak and V. Sashuk, *ChemCatChem*, 2021, **13**, 506–513.
12 W. Szymański, J. M. Beierle, H. A. V. Kistemaker, W. A. Velema and B. L. Feringa, *Chem. Rev.*, 2013, **113**, 6114–6178.
13 P. Kobauri, F. J. Dekker, W. Szymanski and B. L. Feringa, *Angew. Chemie*, 2023, **62**, e202300681.
14 M. J. Fuchter, *J. Med. Chem.*, 2020, **63**, 11436–11447.
15 J. Morstein and D. Trauner, *Curr. Opin. Chem. Biol.*, 2019, **50**, 145–151.
16 M. Heilemann, P. Dedecker, J. Hofkens and M. Sauer, *Laser Photonics Rev.*, 2009, **3**, 180–202.

View Article Online
DOI: 10.1039/D5SC02467F

17 B. Roubinet, M. Weber, H. Shojaei, M. Bates, M. L. Bossi, V. N. Belov, M. Irie and S. W. Hell, *J. Am. Chem. Soc.*, 2017, **139**, 6611–6620.

18 C. Li, K. Xiong, Y. Chen, C. Fan, Y. L. Wang, H. Ye and M. Q. Zhu, *ACS Appl. Mater. Interfaces*, 2020, **12**, 27651–27662.

19 D. Kim, A. Aktalay, N. Jensen, K. Uno, M. L. Bossi, V. N. Belov and S. W. Hell, *J. Am. Chem. Soc.*, 2022, **144**, 14235–14247.

20 M. Mansø, A. U. Petersen, Z. Wang, P. Erhart, M. B. Nielsen and K. Moth-Poulsen, *Nat. Commun.*, 2018, **9**, 1945.

21 A. Gonzalez, Q. Qiu, J. Usuba, J. Wan and G. G. D. Han, *ACS Mater. Au*, 2024, **4**, 30–34.

22 Q. Qiu, Q. Qi, J. Usuba, K. Lee, I. Aprahamian and G. G. D. Han, *Chem. Sci.*, 2023, **14**, 11359–11364.

23 T. J. B. Zähringer, N. P. Lopez, R. Schulte, M. Schmitz, H. Ihmels and C. Kerzig, *Angew. Chemie Int. Ed.*, 2025, **64**, e202414733.

24 A. Gonzalez, M. Odaybat, M. Le, J. L. Greenfield, A. J. P. White, X. Li, M. J. Fuchter and G. G. D. Han, *J. Am. Chem. Soc.*, 2022, **144**, 19430–19436.

25 J. Andréasson, U. Pischel, S. D. Straight, T. A. Moore, A. L. Moore and D. Gust, *J. Am. Chem. Soc.*, 2011, **133**, 11641–11648.

26 X. Chai, Y. X. Fu, T. D. James, J. Zhang, X. P. He and H. Tian, *Chem. Commun.*, 2017, **53**, 9494–9497.

27 H. Zheng, W. Zhou, M. Yuan, X. Yin, Z. Zuo, C. Ouyang, H. Liu, Y. Li and D. Zhu, *Tetrahedron Lett.*, 2009, **50**, 1588–1592.

28 S. Molla and S. Bandyopadhyay, *J. Mater. Chem. C*, 2024, **12**, 17511–17518.

29 C. Petermayer and H. Dube, *Acc. Chem. Res.*, 2018, **51**, 1153–1163.

30 C. Y. Huang and S. Hecht, *Chem. - A Eur. J.*, 2023, **29**, e202300981.

31 C. Y. Huang, A. Bonasera, L. Hristov, Y. Garmshausen, B. M. Schmidt, D. Jacquemin and S. Hecht, *J. Am. Chem. Soc.*, 2017, **139**, 15205–15211.

32 K. Kuntze, J. Viljakka, M. Virkki, C. Y. Huang, S. Hecht and A. Priimagi, *Chem. Sci.*, 2023, **14**, 2482–2488.

33 S. Samanta, A. A. Beharry, O. Sadovski, T. M. McCormick, A. Babalhavaeji, V. Tropepe and G. A. Woolley, *J. Am. Chem. Soc.*, 2013, **135**, 9777–9784.

34 M. Dong, A. Babalhavaeji, S. Samanta, A. A. Beharry and G. A. Woolley, *Acc. Chem. Res.*, 2015, **48**, 2662–2670.

35 M. Gao, D. Kwaria, Y. Norikane and Y. Yue, *Nat. Sci.*, 2023, **3**, e20220020.

36 L. N. Lameijer, S. Budzak, N. A. Simeth, M. J. Hansen, B. L. Feringa, D. Jacquemin and W. Szymanski, *Angew. Chemie - Int. Ed.*, 2020, **59**, 21663–21670.

37 T. Dang, Z. Y. Zhang and T. Li, *J. Am. Chem. Soc.*, 2024, **146**, 19609–19620.

38 C. E. Weston, R. D. Richardson, P. R. Haycock, A. J. P. White and M. J. Fuchter, *J. Am. Chem. Soc.*, 2014, **136**, 11878–11881.

39 A. K. Gaur, D. Gupta, A. Mahadevan, P. Kumar, H. Kumar, D. N. Nampoothiry, N. Kaur, S. K. Thakur, S. Singh, T. Slanina and S. Venkataramani, *J. Am. Chem. Soc.*, 2023, **145**, 10584–10594.

40 Y. He, Z. Shangguan, Z. Zhang, M. Xie, C. Yu and T. Li, *Angew. Chemie*, 2021, **133**, 16675–16682.

41 B. F. Lui, N. T. Tierce, F. Tong, M. M. Sroda, H. Lu, J. Read De Alaniz and C. J. Bardeen, *Photochem. Photobiol. Sci.*, 2019, **18**, 1587–1595.

42 C. A. Reyes, H. J. Lee, C. Karanovic and E. Picazo, *Nat. Commun.*, 2024, **15**, 5533.

43 M. Clerc, S. Sandlass, O. Rifaie-Graham, J. A. Peterson, N. Bruns, J. Read de Alaniz and L. F. Boesel, *Chem. Soc. Rev.*, 2023, **52**, 8245–8294.

44 S. Hatano, T. Horino, A. Tokita, T. Oshima and J. Abe, *J. Am. Chem. Soc.*, 2013, **135**, 3164–3172.

45 H. Ito, S. Tanaka, K. Mutoh and J. Abe, *Org. Lett.*, 2020, **22**, 5680–5684.

46 H. Ito, K. Mutoh and J. Abe, *J. Am. Chem. Soc.*, 2023, **145**, 6498–6506.

47 J. Wu, L. Kreimendahl, S. Tao, O. Anhalt and J. L. Greenfield, *Chem. Sci.*, 2024, **15**, 3872–3878.

48 J. Wu, L. Kreimendahl and J. L. Greenfield, *Angew. Chemie - Int. Ed.*, 2024, **64**, e202415464.

49 J. Wu and J. L. Greenfield, *J. Am. Chem. Soc.*, 2024, **146**, 20720–20727.

50 M. M. Lerch, M. J. Hansen, W. A. Velema, W. Szymanski and B. L. Feringa, *Nat. Commun.*, 2016, **7**, 12054.

51 T. Saßmannshausen, A. Kunz, N. Oberhof, F. Schneider, C. Slavov, A. Dreuw, J. Wachtveitl and H. A. Wegner, *Angew. Chemie - Int. Ed.*, 2024, **63**, e202314112.

52 P. M. Greißel, Z. W. Schroeder, D. Thiel, M. J. Ferguson, T. Clark, D. M. Guldi and R. R. Tykwinski, *J. Am. Chem. Soc.*, 2024, **146**, 10875–10888.

53 L. Köttner and H. Dube, *Angew. Chemie Int. Ed.*, 2024, **63**, e202409214.

54 J. Sheng, J. Perego, S. Bracco, P. Cieciórski, W. Danowski, A. Comotti and B. L. Feringa, *Angew. Chemie - Int. Ed.*, 2024, **63**, e202404878.

55 D. Bléger, S. Hecht, *Angew. Chemie - Int. Ed.*, 2015, **54**, 11338–11349.

56 Z. Zhang , W. Wang , M. O'Hagan , J. Dai , J. Zhang and H. Tian , *Angew. Chem., Int. Ed.*, 2022, **61** , e202205758

57 D. Dattler, G. Fuks, J. Heiser, E. Moulin, A. Perrot, X. Yao and N. Giuseppone, *Chem. Rev.*, 2020, **120**, 310–433.

58 P. E. Swathi Krishna, V. V. Dev, R. Ramakrishnan and M. Hariharan, *ChemPhysChem*, 2022, **23**, e202200045.

59 H. Dube and J. Rebek, *Angew. Chemie - Int. Ed.*, 2012, **51**, 3207–3210.

60 M. Li, S. Yang, W. Liang, X. Zhang and D. Qu, *Dye. Pigment.*, 2019, **166**, 239–244.

61 G. R. Wilson, K. C. Park, G. C. Thaggard, C. R. Martin, A. R. Hill, J. Haimerl, J. Lim, B. K. P. Maldeni Kankanamalage, B. J. Yarbrough, K. L. Forrester, R. A. Fischer, P. J. Pellechia, M. D. Smith, S. Garashchuk and N. B. Shustova, *Angew. Chemie - Int. Ed.*, 2023, **62**, e202308715.

62 V. X. Truong, J. Bachmann, A. N. Unterreiner, J. P. Blinco and C. Barner-Kowollik, *Angew. Chemie - Int. Ed.*, 2022, **61**, e202113076.

63 M. Dowds, S. G. Stenspil, J. H. de Souza, B. W. Laursen, M. Cacciarini and M. B. Nielsen, *ChemPhotoChem*, 2022, **6**, e202200152.

64 Z. Ziani, F. Loiseau, E. Lognon, M. Boggio-Pasqua, C. Philouze, S. Cobo and G. Royal, *Chem. - A Eur. J.*, 2021, **27**, 16642–16653.

65 S. Cobo, F. Lafolet, E. Saint-Aman, C. Philouze, C. Bucher, S. Silvi, A. Credi and G. Royal, *Chem. Commun.*, 2015, **51**, 13886–13889.

66 A. Credi, V. Balzani, S. J. Langford and J. F. Stoddart, *J. Am. Chem. Soc.*, 1997, **119**, 2679–2681.

67 A. P. De Silva, H. Q. N. Gunaratne, T. Gunnlaugsson, A. J. M. Huxley, C. P. McCoy, J. T. Rademacher and T. E. Rice, *Chem. Rev.*, 1997, **97**, 1515–1566.

68 M. P. Bhat, S. Vinayak, J. Yu, H. Y. Jung and M. Kurkuri, *ChemistrySelect*, 2020, **5**, 13135–13143.

69 P. A. De Silva, N. H. Q. Gunaratne and C. P. McCoy, *Nature*, 1993, **364**, 42–44.

70 E. H. Witlicki, C. Johnsen, S. W. Hansen, D. W. Silverstein, V. J. Bottomley, J. O. Jeppesen, E. W. Wong, L. Jensen and A. H. Flood, *J. Am. Chem. Soc.*, 2011, **133**, 7288–7291.

71 M. Jacquet, L. M. Uriarte, F. Lafolet, M. Boggio-Pasqua, M. Sliwa, F. Loiseau, E. Saint-Aman, S. Cobo and G. Royal, *J. Phys. Chem. Lett.*, 2020, **11**, 2682–2688.

72 Z. Ziani, S. Cobo, F. Loiseau, D. Jouvenot, E. Lognon, M. Boggio-Pasqua and G. Royal, *JACS Au*, 2023, **3**, 131–142.

View Article Online
DOI: 10.1039/D5SC02467F

73 R. H. Mitchell and T. R. Ward, *Tetrahedron*, 2001, **57**, 3689–3695.

View Article Online
DOI: 10.1039/D5SC02467F

The data supporting this article have been included as part of the Supplementary Information.